Provided for non-commercial research and education use.
Not for reproduction, distribution or commercial use.

This article appeared in a journal published by Elsevier. The attached copy is furnished to the author for internal non-commercial research and education use, including for instruction at the authors institution and sharing with colleagues.

Other uses, including reproduction and distribution, or selling or licensing copies, or posting to personal, institutional or third party websites are prohibited.

In most cases authors are permitted to post their version of the article (e.g. in Word or Tex form) to their personal website or institutional repository. Authors requiring further information regarding Elsevier's archiving and manuscript policies are encouraged to visit:

http://www.elsevier.com/copyright

Author's personal copy

Surface Science 602 (2008) 2069–2077

Contents lists available at ScienceDirect

Surface Science

journal homepage: www.elsevier.com/locate/susc

Extracting the Ag surface and volume loss functions from reflection electron energy loss spectra

M.R. Went [a], M. Vos [a,*], W.S.M. Werner [b]

[a] Atomic and Molecular Physics Laboratory, Research School of Physical Sciences and Engineering, The Australian National University, Canberra 0200, Australia
[b] Institut für Allgemeine Physik, Vienna University of Technology, Wiedner Hauptstraße 8–10, A 1040 Vienna, Austria

ARTICLE INFO

Article history:
Received 22 January 2008
Accepted for publication 14 April 2008
Available online 22 April 2008

Keywords:
Reflection electron energy loss spectroscopy
Silver
Dielectric function
Surface electronic phenomena

ABSTRACT

Reflection electron energy loss spectra have been measured for silver using incoming electrons with energies between 5 and 40 keV, in a surface and volume-sensitive geometry. Bulk and surface loss functions are extracted from these data and various consistency checks are applied to the obtained loss functions. Depositing minute amounts of Al onto the Ag surface causes a severe reduction in surface features. The intensity of the surface feature seems now to increase as the probe energy is increased. A mechanism by which this can occur is discussed. The relation between the bulk loss function and the dielectric function is discussed, and a comparison with the results of transmission electron energy loss spectra and optical data is made.

© 2008 Elsevier B.V. All rights reserved.

1. Introduction

Reflection electron energy loss spectroscopy (REELS) has attracted interest for over 50 years [1]. It was established early that the spectra contain information about surface and volume loss features [2,3], and that there is a close relation between these features and the dielectric function of the material. Knowledge of the dielectric function is important, not only to describe the interaction of photons and energetic electrons with a material, but also for the description of electron–electron correlation effects in ab initio calculations, as the electron–electron interaction is effectively reduced by screening due to the medium, and this reduction is described by the dielectric function. Experimental information about the dielectric function is thus extremely important.

However, extracting the dielectric function from a REELS spectrum turns out to be a real challenge and has attracted a lot of theoretical interest [4,5]. A main hurdle is that simultaneous understanding of both surface and bulk loss processes is required and this problem has been addressed in several papers in the last few years (see e.g. [6–10]). It has even been suggested that at the lowest energies interference between volume and surface oscillations will make separation impossible [5,11,12], and a REELS spectra cannot be considered to be a simple linear combination of surface and volume components. We assume that this problem does not occur in the present measurements which are at relatively high energies (5 keV and above).

Silver is a ideal material for study as the REELS spectrum is feature-rich and contains a very strong peak in the vicinity of 3.7 eV, which is due to both surface (3.63 eV) and volume (3.78 eV) plasmons. These surface plasmon features play an important role in the development of plasmonic devices [13,14]. Surface and volume plasmons were resolved in high-resolution transmission measurements [15], but reflection electron energy loss measurements usually lack the required resolution. While our current experimental resolution prohibits us from resolving the two components individually, by changing the energy and geometry of the incident electrons we are able to reduce or enhance either contributions. At larger energy loss values there is second plasmon near 8 eV followed by additional structure due to interband transitions.

At an interface a different loss mode is possible. For a free electron material the interface plasmon is at an energy

$$\omega_i = \frac{\omega_{\mathrm{pl}}}{\sqrt{1+\epsilon}}, \tag{1}$$

with ω_{pl} the plasmon energy and ϵ the dielectric constant of the overlayer material [16]. For a surface the dielectric constant is that of the adjacent vacuum ($\epsilon = 1$) and the surface plasmon is at $\frac{1}{\sqrt{2}}\omega_{\mathrm{pl}}$. As noticed before for silver the bulk and surface plasmon are much closer in energy than these values, due to the influence of the 4d bands. Daniels studied the influence of a carbon overlayer on Ag [17]. Near the Ag plasmon energy the dielectric constant of carbon is >1, and the surface plasmon shifts to lower energy loss values after carbon deposition (and becomes much more strongly damped). Here, we investigate what happens, if we deposit aluminum on an silver surface. Near 4 eV the Al dielectric function is

* Corresponding author.
E-mail address: maarten.vos@anu.edu.au (M. Vos).

0039-6028/$ - see front matter © 2008 Elsevier B.V. All rights reserved.
doi:10.1016/j.susc.2008.04.011

Author's personal copy

severely negative, and $1+\epsilon$ becomes negative and the imaginary value of ω_i in Eq. (1) suggests that no interface plasmon will exist.

The surface excitation parameter (SEP) is the average number of surface excitations an electron experiences in crossing the vacuum–solid interface once. The SEP for medium-energy electrons is given in Ref. [18] as

$$P_s(\theta, E_0) = \frac{a}{\sqrt{E_0}\cos\theta}, \tag{2}$$

where E_0 is the incident electron energy, θ is the angle of the surface crossing with respect to the surface normal and a is a material parameter, being equal to 2.896 $eV^{1/2}$ for free electron materials. Thus one can change the probability of exciting a surface plasmon by either changing the probe electron energy or by changing the angle of incidence of the incident beam to the surface. It is this property that enables to distinguish between volume and surface features of the energy loss spectra. As the excitation probability scales as $1/\sqrt{E_0}$ one has to increase the energy 4-fold to get a reduction of a factor of 2 of the fraction of detected electrons that experienced surface losses.

Note that the surface (and interface) plasmons are not purely an additional loss feature. Already the early theory by Ritchie [3] predicted a corresponding decrease in the excitation probability of a bulk plasmon near the surface, that was recently demonstrated by analysis of experimental REELS [19]. The width of the surface scattering zone is given by v/ω_s [3], where v is the speed of the electron as it crosses the surface and ω_s is the surface plasmon frequency. As a consequence, the depth over which the bulk plasmon excitation is reduced due to the surface, increases with the square root of the energy. The thickness of the overlayer required to replace the surface plasmon by an interface plasmon increases with energy as well [16].

In the past theory and experiment were confronted with each other using Monte Carlo simulations, reconstructing the experiment and using theoretical estimates of the loss functions etc., as an input. For example, in an extensive study Ding et al. [20] compared theoretical depth-dependent loss function with experimental REELS spectra using Monte Carlo simulations. They identified another surface loss feature, besides the sharp loss feature near 3.7 eV. This feature, near 7.5 eV, is much broader in energy, but also displays a maximum in cross section at the surface.

Recently, a new scheme was developed to determine the single scattering surface and volume loss functions directly from the experimental data [21]. This calculation requires as input two loss spectra for which the contributions due to surface and volume loss functions are different, for example loss functions measured at different energies and or geometrical configurations. The technique involves deconvoluting the loss function to remove multiple scattering while simultaneously separating surface and volume components. This method was successfully applied to Ag and Au using high-energy REELS data from the spectrometer at the Australian National University [22,23]. This spectrometer can be used to measure REELS spectra in an energy range between 5 and 40 keV, and is hence ideally suited to provide the input data for the extraction of the surface and volume excitation function by the aforementioned theory. Further the complex dielectric function was derived from the volume and surface loss function, by fitting it with a set of Drude–Lindhard oscillators [23]. The dielectric function obtained in this way satisfies Kramers–Kronig relation and the bulk loss function is given by $\mathrm{Im}\{-1/\epsilon\}$ and the surface loss function by $\mathrm{Im}\{(\epsilon-1)^2/\epsilon(\epsilon+1)\}$. The REELS-derived dielectric function appeared to be in better agreement with density-functional theory calculations than the dielectric function obtained by optical means [24].

The method developed by Werner to derive the loss functions from a REELS spectrum is far from trivial. If it can be validated then REELS can become an important tool to derive dielectric functions over a wide energy range, and a large variety of samples. Thus, it is highly desirable to be able to judge the validity of the obtained surface and volume loss functions by experiments. This paper tries to explore to what extent this is possible for the case of silver, by studying the effects of changing energy and geometry, as well as the influence of adding a thin overlayer to silver.

2. Experiment

The measurements presented in this work were performed on the high energy electron spectrometer at the Australian National University, shown in Fig. 1. The electron energy analyzers have been described in detail elsewhere [25] and are operated at a pass energy of 200 eV. Measurement can be done with either gun A or gun B. Both guns are equipped with a BaO cathode, operating at low temperatures to minimize the energy spread. The cathode is held at a potential of −500 V. The sample is positioned in a high voltage hemisphere which is held at the required voltage (ie., 4.5, 9.5, 19.5 and 39.5 kV). Thus electrons with an energy of 5, 10, 20 and 40 keV are incident on the target. Electrons which scatter from the target are decelerated and focussed into the entrance of a hemispherical electron energy analyzer. Ripple and drift of the main high voltage power supply do not affect the resolution of the experiment, as it is used both to accelerate the incoming electrons and decelerate the scattered electrons, and hence does not change the energy of the detected electron inside the hemispherical analyzer. The analyzer is held at a (comparatively low) voltage such that electrons with the desired energy pass through the analyzer and are detected by a pair of micro-channel plates followed by a resistive anode. facilitating two dimensional analysis of the electron position. Electrons over an energy range of 30 eV can be detected simultaneously and analyzed accurately for their energy. The combined resolution of gun and analyzer is always better than 0.5 eV.

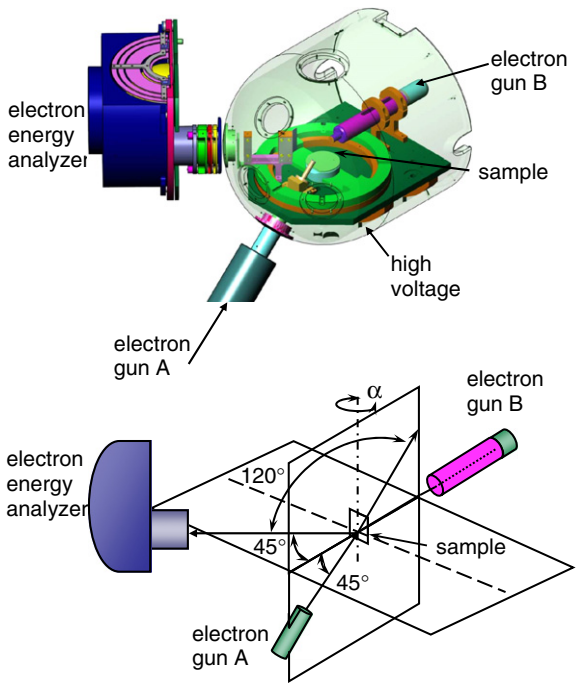

Fig. 1. Outline of experimental apparatus (top). Schematic of the experiment showing the relative positions of the two electron guns and sample position (bottom). The sample can rotate around the vertical axis over an angle α. For the sample orientation drawn here $\alpha = 0°$.

Author's personal copy

The spectra obtained with the two electron guns differ, as their geometry is different. Gun A is positioned at 45° below the horizontal plane (see Fig. 1), and electrons which emerge in the horizontal plane at an angle of 45° with the vertical plane containing the gun, are collected and analyzed by the hemispherical electron energy analyzer. The scattering angle is then 120°. The sample surface normal is both in the horizontal plane containing the analyzer and in the vertical plane containing the gun (the sample is in the position sketched in Fig. 1, i.e., $\alpha = 0$). Measurements were done in this configuration are considered to be relatively 'volume-sensitive' as neither the incoming or outgoing trajectories are glancing. Measurements done with gun B have the incident and detected electrons in the same plane and the scattering angle is 45°. The sample is then rotated ($\alpha = 112.5°$), and in this configuration the incoming and outgoing trajectories are relatively glancing (22.5° to the surface). These measurements are thus 'surface sensitive' and the SEP is larger. Furthermore, by changing the electron energy over a 5–40 keV range the inelastic mean free path and hence the surface sensitivity can be varied.

The silver samples are prepared from 99.99% purity silver wire, which has been formed into disks. The surface is then cleaned by either ion bombardment with Xe ions or by evaporating a new surface from the same wire. Aluminium is deposited by evaporation of 99.95% purity aluminium wire from a resistively heated BN crucible. The base pressure of the preparation areas are below 5×10^{-9} torr and samples are moved from these areas to the measurement chamber $<1 \times 10^{-10}$ torr immediately after they are prepared to ensure surface quality is maintained.

3. Extracting the surface and volume loss function from Ag REELS spectra

The decomposition of REELS data into surface and bulk components needs to take into account that an electron can create any number of surface and bulk excitations (n_s and n_b, respectively), and determining the frequency that any combination of n_s and n_b occurs requires detailed knowledge of both elastic and inelastic scattering processes. The shape of the contribution of events with (n_s, n_b) surface and volume losses is the (n_s, n_b)-fold convolution of the distribution of surface (w_s) and bulk (w_b) losses in an individual collision. The observed spectrum is then proportional to the sum of these (n_s, n_b)-fold convolutions, weighted by the number of electrons arriving at the detector after experiencing (n_s, n_b) losses occur, the so-called partial intensities C_{n_b,n_s}. Commonly, a REELS spectrum is divided by the area of the elastic peak (i.e., the zero-order partial intensity $C_{0,0}$) for normalization purposes, so that the relative number of electrons that have participated in (n_s, n_b) surface and bulk collisions is then described by the reduced partial intensities $\gamma_{n_b,n_s} = C_{n_b,n_s}/C_{n_b=0,n_s=0}$ and the elastic peak area is unity after normalization, $\gamma_{0,0} \equiv 1$. When two loss spectra with a different sequence of partial intensities are measured, the single scattering loss distributions $w_b(T)$ and $w_s(T)$ can be found by means of the formula [26]:

$$w_{s,b}(T) = \sum_{k=0}^{2}\sum_{l=0}^{2} a_{k,l} Y_{k,l}(T) - \int_{T'=0}^{T} \sum_{k=0}^{2}\sum_{l=0}^{2} b_{k,l} Y_{k,l}(T-T') w(T')\,\mathrm{d}T', \tag{3}$$

where the quantity $Y_{k,l}(T)$ is the (k,l)th order cross convolution of the two REELS spectra and the coefficients $a_{k,l}$ and $b_{k,l}$ are a function of the reduced partial intensities and $b_{k,l}$ are different for the surface $w_s(T)$ and bulk $w_b(T)$ loss distribution. The bulk and surface partial intensities are uncorrelated to a good approximation [19]:

$$C_{n_b,n_s} = C_{n_b} \times C_{n_s}, \tag{4}$$

implying that the bulk and surface partial intensities C_{n_b} and C_{n_s} can be calculated separately. Plural surface scattering is commonly assumed to follow Poisson statistics:

$$C_{n_s}(\theta) = \frac{P_s(\theta)^{n_s}}{n_s!} \mathrm{e}^{-P_s(\theta)}. \tag{5}$$

The volume partial intensities C_{n_b} represent the number of electrons that arrive in the detector after being n_b-fold inelastically scattered in the solid and are given by an integral over all possible lengths of the paths s taken by the particle in the solid, $Q(s)$, multiplied with the probability for suffering n_b collisions as function of the pathlength [6]:

$$C_{n_b} = \int_0^\infty \left(\frac{s}{\lambda_i}\right)^{n_b} \frac{\mathrm{e}^{-s/\lambda_i}}{n_b!} Q(s)\,\mathrm{d}s. \tag{6}$$

Examples of calculations for the pathlength distributions corresponding to the present experiments are shown in Fig. 2. These quantities were calculated with a Monte Carlo simulation [7]. Elastic scattering cross sections of silver, being the only quantities required as input for these calculations, are well established at these high energies, and largely independent of details of the atomic potential used [27].

The corresponding reduced volume partial intensities calculated with Eq. (6) are presented in Fig. 3, using the TPP-2 values as a rough estimate of the inelastic mean free path [28]. Note that we use the TPP-2 formula here at much higher electron energies than originally intended in Ref. [28], but there is no clear physical reason why the formula would fail dramatically at higher energies. Table 1 summarizes some of the relevant values of parameters used for the transport calculations. Note that for the reduced volume partial intensity $\gamma_1 = C_{n_b=1,n_s=0}/C_{n_b=0,n_s=0}$, the accuracy of the inelastic mean free path used is almost completely irrelevant, a rough estimate is sufficient. This can be seen by employing the common rules of error propagation to Eq. (6). For the reduced par-

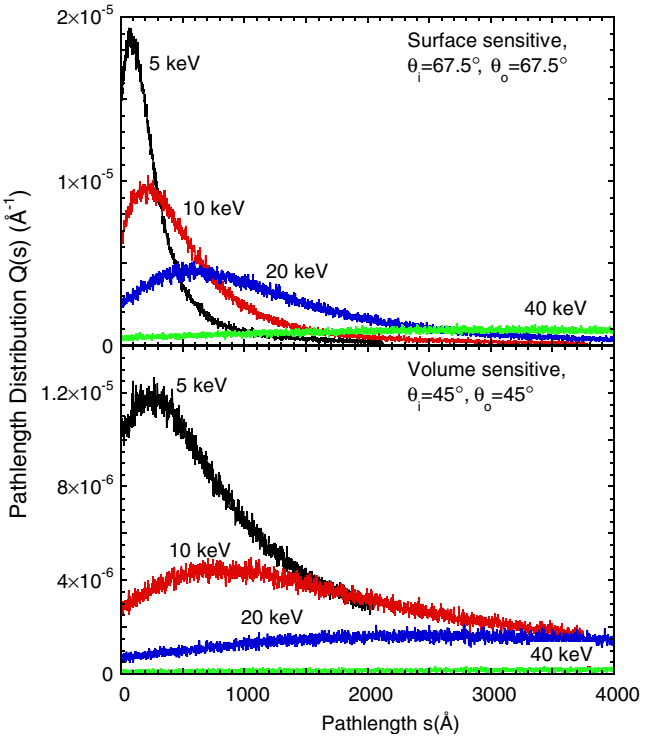

Fig. 2. Pathlength distributions for electron backscattering for various energies and for the surface- (top) and volume- (bottom) sensitive geometry as calculated by means of a Monte Carlo simulation.

Author's personal copy

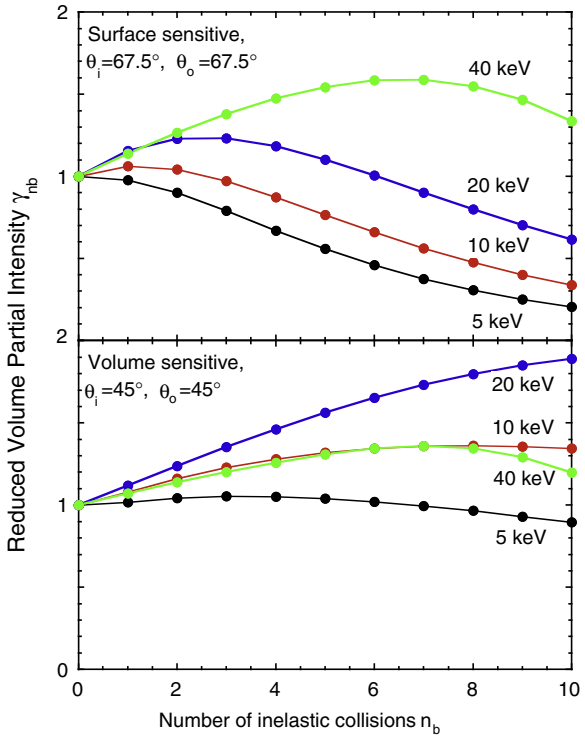

Fig. 3. (Bulk) partial intensities corresponding to the pathlength distributions shown in Fig. 2 calculated by means of Eq. (6) for the surface sensitive (top) and bulk sensitive (bottom) geometry.

Table 1
Values of some characteristic lengths for electron transport in Ag for energies between 5 and 40 keV

E (keV)	λ_i (Å)	λ_e (Å)	λ_{tr} (Å)	v/ω_s (Å)
5	53	18	281	69
10	94	27	785	97
20	168	41	2304	137
40	307	160	13158	196

λ_i: Inelastic mean free path, λ_e: elastic mean free path, λ_{tr}: transport mean free path, v/ω_s: width of the surface scattering zone for the 3.87 eV surface plasmon in Ag. For the Al surface plasmon the width of the surface scattering zone is a factor of about 2.5 smaller.

tial intensities one finds that an uncertainty $\Delta\lambda$ in the IMFP leads to an error in the first-order reduced partial intensity given by

$$\frac{\Delta\gamma_1}{\gamma_1} = \left|\frac{\Delta\lambda}{\lambda}\right| |1-\gamma_1|. \quad (7)$$

Since the pathlength distributions are very broad compared to the value of the IMFP (see Table 1) the difference between the reduced partial intensities of subsequent order is always considerable smaller than unity, implying that γ_1 is always quite close to unity. In consequence, the error in the partial intensities due to an uncertainty in the IMFP is always negligible for a reasonably realistic estimate of the IMFP. For the SEP, the empirical predictive formula in Ref. [29] was used from which the surface partial intensities were calculated.

Measurements of the REELS spectra were performed in both geometries (using gun A and gun B) at four energies 5, 10, 20, 40 keV. The Ag elastic peak is aligned with 0 eV and all spectra are normalized to an elastic peak area of 1. The spectra can roughly be described by a surface/volume component around 4 and 8 eV with volume transitions between 4 and 150 eV. Above 50 eV most of the intensity consists of multiple bulk and or surface losses.

Examples of spectra, obtained using gun A and gun B, are given in Fig. 4 as well as the obtained loss functions, using Eq. (3) [21]. It is important to choose the difference in energy between the two spectra, used as input, as large as possible as the extraction of the surface and volume loss function requires that both processes contribute in clearly different relative intensity to both spectra. The spectra taken with gun A (a rather volume-sensitive geometry) the surface excitations are not too strong at either energies. Also the statistics of the spectra taken with gun A is generally not as good as the statistics of spectra taken with gun B, as the (elastic) differential cross section at 45° is, at these energies, much larger than the differential cross section at 120° scattering angle. For these reasons the error in the extracted surface loss function from spectra taken with gun A is relatively large and this is reflected in

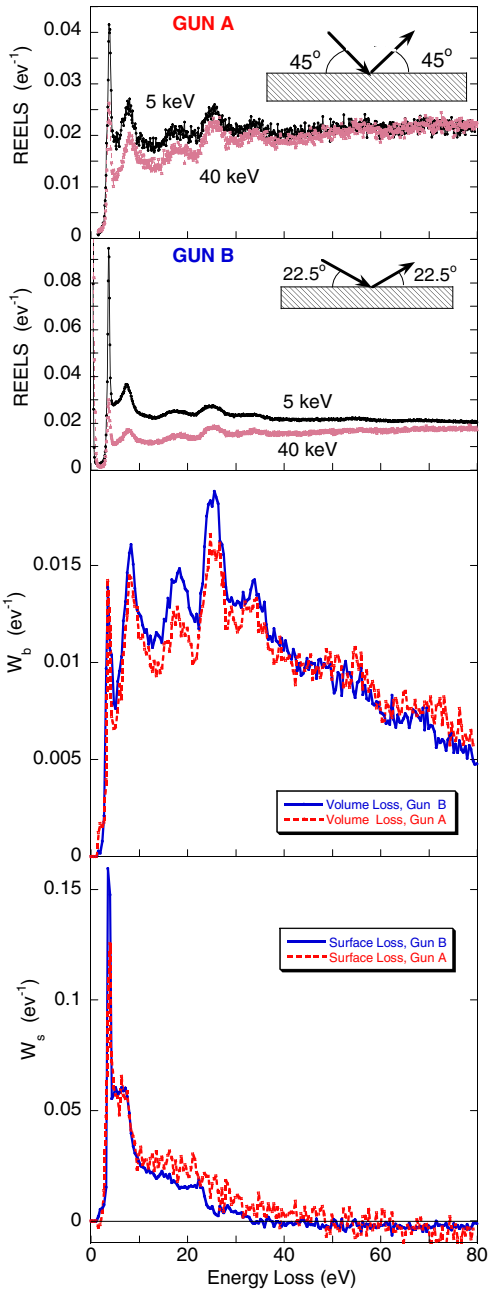

Fig. 4. Measured loss spectrum of Ag at 40 and 5 keV obtained using gun A and B (top panels). The derived single (surface and volume) loss functions, as derived independently for both geometries are shown in the 3rd and 4th panel, respectively.

Author's personal copy

the 'noisy' curves obtained. The bulk loss function, derived from this measurement should be fairly reliable, as the surface losses contribute, especially in the 40 keV spectra, only modestly. The differences in the spectra taken with gun B (in a surface sensitive geometry) are larger, the 5 keV measurement is dominated by surface excitations. The obtained surface loss function from this measurement is indeed less 'noisy' than the one obtained with gun A and should be more reliable. The two estimates of the surface and bulk loss function of gun A and B are completely independent, and the level of agreement obtained is thus a good indication of the validity of both experiment and theory. Qualitatively the agreement is good, peaks appear in the surface and bulk loss function in the same energy position in both measurements. However, there are slight variations in the intensity of the loss features, and this difference can be viewed as an estimate of the combined error of the experiment and theoretical calculation. The main discrepancy is in the intensity in the 20–30 eV region. Note that the bulk loss feature is here more intense for gun B, whereas the surface loss function is in this energy range more intense for gun A.

A different approach is to compare the bulk loss function with that obtained using the procedure described by Tougaard and Chorkendorff (TC) [4]. It is a straightforward procedure, without adjustable constants but it does not take into account surface excitations. Hence, its results are expected to be poor under surface sensitive conditions, but maybe reasonable for 40 keV measurement in a volume-sensitive geometry. The result of this analysis is given in Fig. 5. The loss function obtained by the TC procedure ('w^{TC}') is clearly dependent on the incoming electron energy E_0 and geometry, and its intensity in the low loss area (where surfaces losses can be expected) is largest for the more surface sensitive geometry. Also in Fig. 5 is shown the volume loss function as obtained in this work. It is not identical to any of the TC results, but clearly for the most volume-sensitive geometry and highest energy the TC result start approaching the current result. Also from this figure it is clear by extrapolation, that for even more volume-sensitive measurements the TC result would be even closer to the present one.

Within the framework of partial intensity analysis (PIA) w^{TC} can be approximated by w^{TC}_{PIA}: a linear combination of the contribution due to the partial intensities $\alpha_{1,0}$, $\alpha_{0,1}$ and $\alpha_{1,1}$ [21]:

$$w^{TC}_{PIA} = \alpha_{1,0} w_b + \alpha_{0,1} w_s - \alpha_{1,1} w_b \otimes w_s. \quad (8)$$

In Fig. 6 we show for the 5 and 40 keV measurements using gun A that indeed the TC result can be described by Eq. (8) and the obtained partial intensities. However, even in the high-energy measurement in the bulk sensitive geometry this analysis indicates that 50% of the feature near 3.7 eV is still related to the surface loss function w_s.

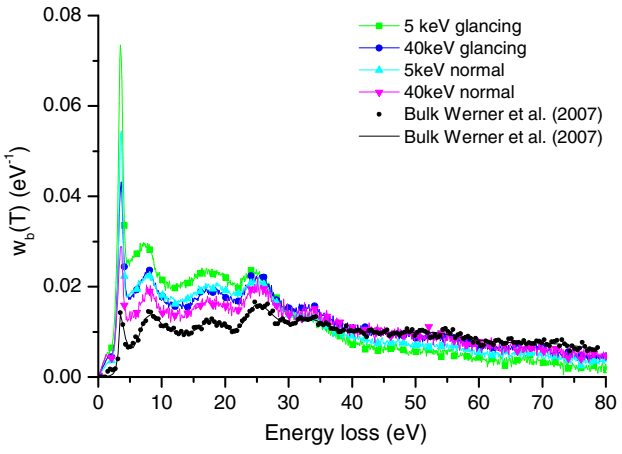

Fig. 5. The result of the Tougaard–Chorkendorff procedure for various energies and geometries, compared to the loss function derived in [23] (black dots) and line (fit of the dots based on a set of Drude–Lindhard oscillators).

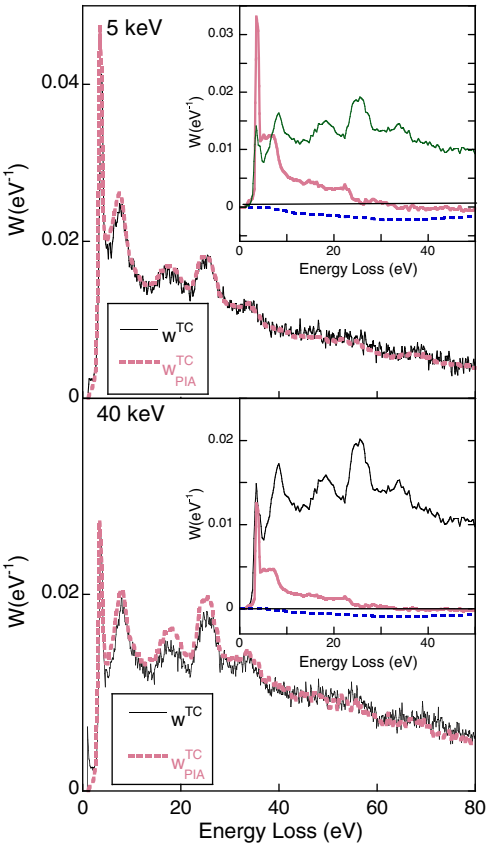

Fig. 6. The comparison of the result of the TC procedure w^{TC} (solid line) and its approximation w^{TC}_{PIA} as given by Eq. (8) (dashed line) for the 5 and 40 keV measurement using gun A. The inserts show the contributions on w_s (thick solid line), w_b (thin solid line) and $w_s \otimes w_b$ to w^{TC}_{PIA} (dashed line). For the 5 keV measurement the contribution of the term proportional to $w_b \otimes w_s$ is significant. The peak in the TC result near 3.8 eV is at 5 keV dominated by contributions of w_s, and even at 40 keV the surface loss contribution is at this energy of the same order as the bulk loss contribution.

From the surface and bulk loss function shown in Fig. 4, it appears clear that a peak near 3.7 eV is present not only in the surface loss function, but also in the bulk loss function. It is obvious that the peak near 3.7 eV is most intense under surface sensitive conditions. Clearly surface excitations are important here and Ding et al. [20] concluded (using lower energy REELS data) that the 3.7 eV peak is for all practical purpose a surface plasmon. It is well known that surface and volume plasmon of Ag should be very close in energy, due to the interaction with the 4 d bands. These peaks have been separated in high-resolution transmission experiments [15] using a monochromatised electron beam. Can we determine from these REELS measurements, without resorting to an extensive mathematical analysis, if a feature near 3.7 eV is present in the bulk loss function. This will be discussed next.

One way to study this is by measuring the area of the 3.7 eV feature as a function of energy. This is done by fitting this part of the measured spectrum with a Gaussian and a Shirley-type background function. As the feature is quite sharp, its area (relative to the elastic peak) does not depend dramatically on details of the assumed background function. The results are shown in Fig. 7. A marked difference of the 3.7 eV peak intensity is found between both geometries. This is expected as the angle of the incoming

Author's personal copy

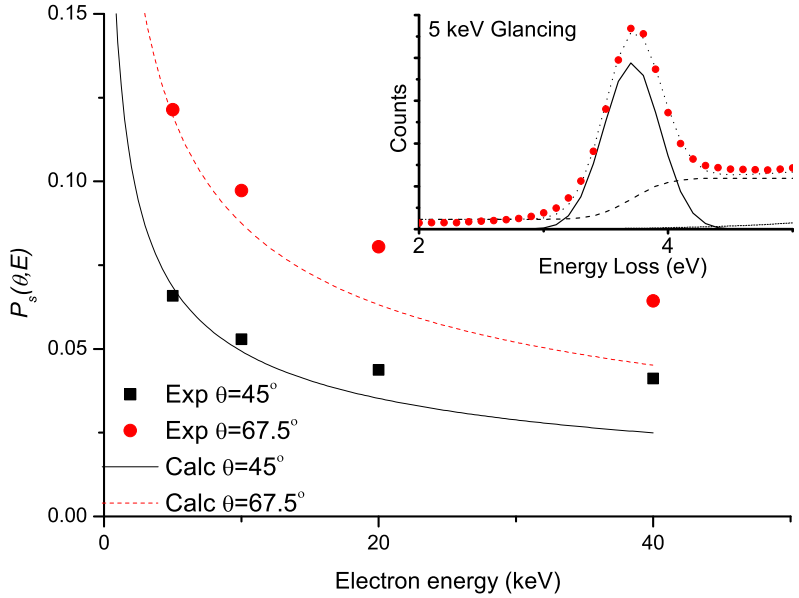

Fig. 7. The probability of a surface excitation in a REELS experiment (two surface crossings, i.e. 2^*SEP as calculated using Eq. (2) compared to $5 \times I_{3.7}/I_0$. ($I_{3.7}$ is the area of the 3.7 eV feature, I_0 the area of the elastic peak.). Solid line and squares are for the bulk sensitive geometry, dashed line and dots for the surface sensitive geometry. The factor of 5 is explained if only 20% of the surface loss function is associated with the sharp feature near 3.7 eV, in reasonable agreement with the shape of the surface loss function shown in Fig. 4. The insert shows the 'background' that was used to extract $I_{3.7}$ from the raw experimental data, for the 5 keV glancing measurement.

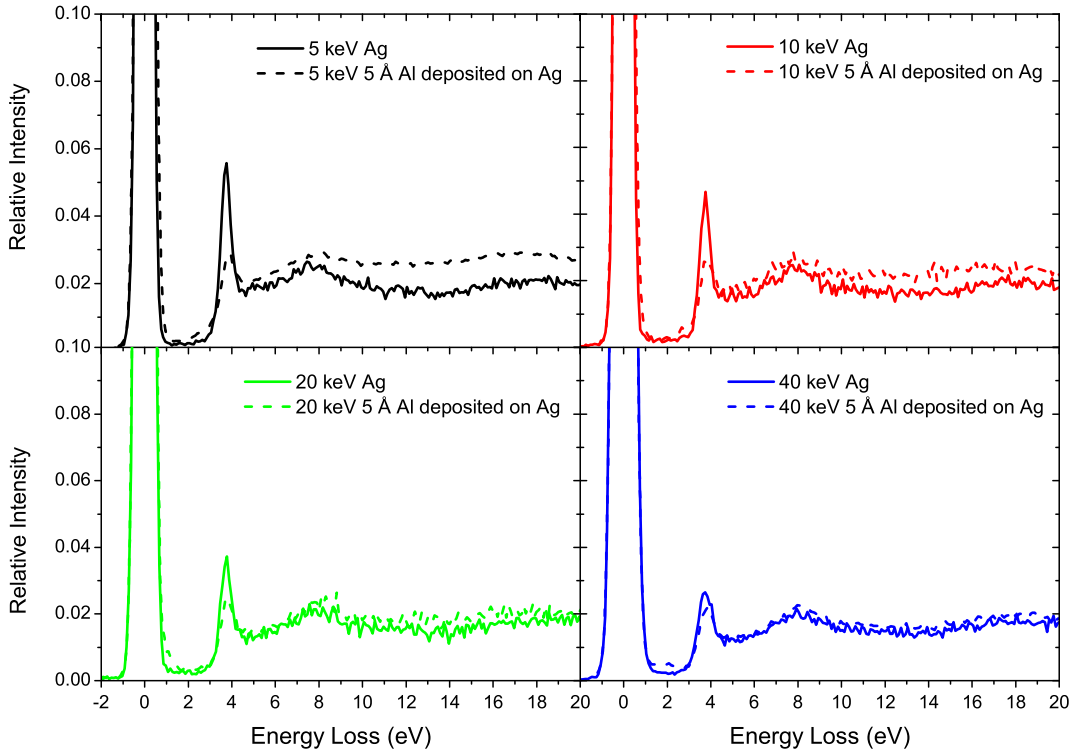

Fig. 8. Spectra of Silver measured with gun A (volume-sensitive geometry). Deposition of 5 Å of Al on a clean surface changes the spectrum, especially the peak near 3.7 eV and low incoming energies.

and scattered electrons to the surface normal (and hence $\cos\theta$ in Eq. (2)) is reduced in the volume-sensitive configuration. If the surface loss function as shown in Fig. 4 is correct then the sharp peak at 3.7 eV forms only a fraction of all the surface excitations. Hence, we cannot compare the total intensity directly with that of Eq. (2), and a scaling factor of 5 was used to get about the right amount of the 3.7 eV feature in both geometries at low energies. This indicates that only ≈20% of the surface loss function is associated with the 3.7 eV feature, in reasonable agreement to the surface loss function of Fig. 4.

The experimentally-found decrease with increasing energy of the 3.7 eV feature is less than that predicted by Eq. (2). This is a clear indication that the 3.7 eV feature is not only due to surface excitations. From the difference in measured and estimated inten-

Author's personal copy

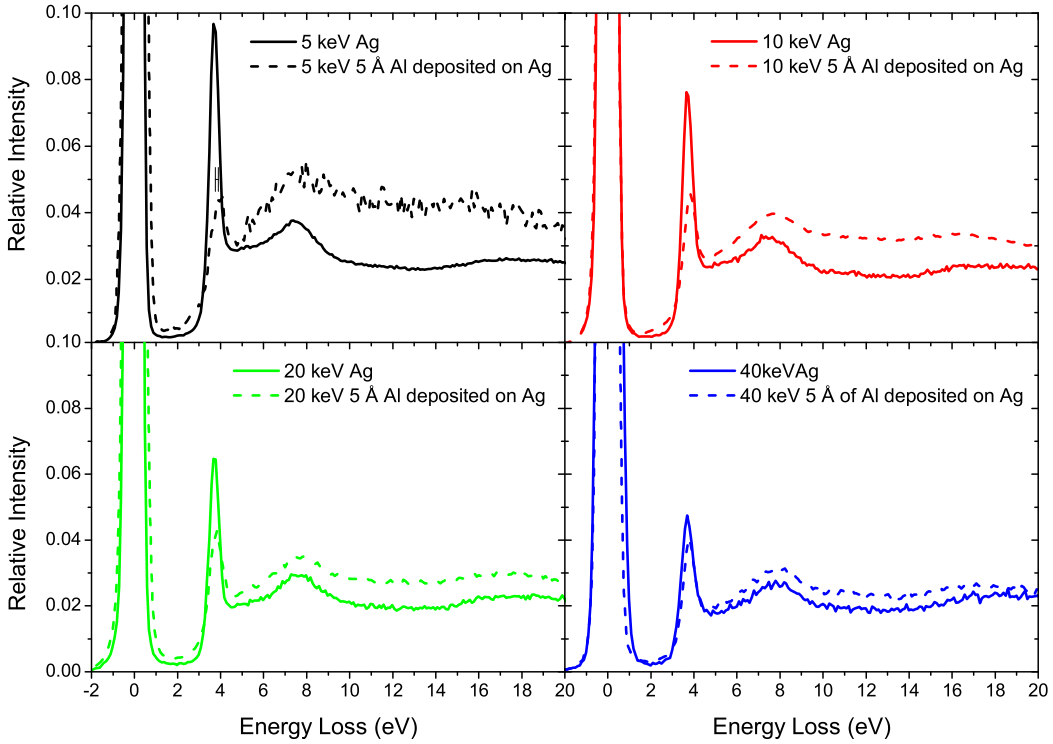

Fig. 9. The same as Fig. 8 but now measured using gun B i.e., in the surface sensitive geometry. The apparent shift of the main peak after Al deposition is indicated in the 5 keV measurement.

sity of the 3.7 eV feature one would estimate that approximately a third of the 3.7 eV peak measured at 40 keV in the volume-sensitive geometry is due to the volume plasmon, in reasonable agreement with the decomposition of w^{TC} shown in Fig. 6. The surface peak around 8 eV is also affected, but due to the larger peak width, variations in its intensity are harder to discern. Thus the presence of a sharp peak in the volume loss function in Fig. 4 near 3.7 eV is consistent with the observed energy dependence of the intensity of the observed 3.7 eV feature.

Another way to change the Ag surface peak is to modify the surface. This was achieved by evaporating 5 Å of aluminium onto the silver surface. This reduces the intensity of the 3.7 eV peak considerably. The effect of Al deposition is largest for the 5 keV surface sensitive geometry. In the volume-sensitive geometry the remaining intensity at 3.7 eV is fairly independent of E_0, which could be seen as an argument that the remaining intensity is due to volume excitations.

Interestingly in the glancing geometry, where the intensity of the 3.7 eV feature was initially much larger at 5 keV, compared to 40 keV, Al deposition leads to a reversal of the energy dependence of the intensity of this peak. Now the 3.7 eV peak is more pronounced for the 40 keV measurement. One explanation is that at 40 keV the 5 Å Al layer is not thick enough to extinguish the Ag surface plasmon, whereas at 5 keV it is. Such a dependence of the required thickness on energy was predicted by Stern and Ferrel [16]. The reason that this reversal is not so evident for the volume-sensitive geometry is that the contribution of the surface plasmon is always quite small, especially at higher energies.

In the measurements where the 3.7 eV intensity changes significantly, one observes also a small shift of the peak position following deposition of 5 Å of aluminium. This shift is of the same order as the separation found for the surface and volume plasmon in transmission EELS experiments (0.15 eV) [15]. This supports the interpretation that the peak near 3.7 eV was before Al deposition mainly a surface excitation, but the remaining intensity after Al deposition is dominated by volume excitations. The magnitude of the shift is indicated in the top left panel of Fig. 9. This shift becomes less noticeable in the higher energy measurements and in the more volume-sensitive measurements. This seems to indicate that, indeed, a significant fraction of the 3.7 eV peak of a clean surface is, at higher energies, due to a volume plasmon.

It has been shown that the "roughness" of a surface can also effect the surface plasmon [30,31]. To eliminate the effect of deposition from the REELS spectra a silver sample was prepared and sputter cleaned. A further silver layer (≈100 Å thick) was deposited on the clean surface. The obtained spectra were identical to that from sputter-cleaned silver surface.

By evaporating Al on Ag we replaced the vacuum-Ag interface by an Al–Ag interface. The surface plasmon becomes an interface plasmon. For Al ϵ_1 is negative near 4 eV, and hence the intensity should shift to higher energies, closer to the energy of the Al plasmon. Indeed an increase in intensity is seen between 8 and 15 eV. This contrasts to the results of Daniels for carbon deposition on Al. For carbon ϵ_1 is larger than 1 at these energies, and one expects based thus a shift of the C–Ag interface plasmon to lower energies compared to the Ag surface plasmon. This is indeed what was seen by Daniels [17].

4. Comparison with optical and transmission electron energy loss measurements

It would be a big step forward, if the results of the decomposition of the REELS measurements could be compared to the outcome of other techniques. The main candidates for this comparison are transmission electron energy loss spectroscopy (EELS) experiments and optical absorption/reflection measurements. Both techniques can be used to measure $\mathrm{Im}\{-1/\epsilon(\omega, q=0)\}$, but there are some problems, if we want to compare the volume loss function with these quantities.

Author's personal copy

During an inelastic excitation the fast electron is deflected over a small angle θ and there is a small momentum transfer q from the medium to the fast electron ($q \approx k\theta$ for small θ). The energy of the excitation tends to change with q (dispersion). This complicates the comparison of our present result with those obtained by transmission electron energy loss experiments and optical means, where usually $q \simeq 0$. The theory is well described in e.g. [32], and we summarize here only some of the essential points.

The cross section decreases with increasing θ and is given by

$$\sigma(\theta) = \frac{c}{\theta_e^2 + \theta^2}, \tag{9}$$

with c a constant and $\theta_e = \omega/2E_0$, with ω the energy of the loss feature. The energy of the excitation is generally also a function of q and changes often like $\omega(q) = \omega_0 + Cq^2$ with C that varies from e.g. 0.6 E_f/ω_0 (plasmon excitations, E_f is the Fermi Energy) to $1/(2m_e)$ (final state a free electron, mass m_e), but negative values of C occur as well, e.g., in the case of Cs [34]. For Ag the dispersion of the first loss features has been determined experimentally [35], and are positive. In a REELS experiment one has no information over θ (as it is obscured by the large angle elastic scattering event(s) required to deflect the electron in the analyzer), hence each energy loss feature contributes to a somewhat extended range of energies.

In transmission electron energy loss experiments the detector (with a very small opening angle) is generally placed at $\theta = 0$ and the resulting loss function corresponds to $\mathrm{Im}\{-1/\epsilon(\omega, q = 0)\}$. Moving the detector away from $\theta = 0$ one observes the dispersion of the loss features. In optical spectroscopy one obtains the real and imaginary part of ϵ at $q = 0$ and calculates from this $\mathrm{Im}\{-1/\epsilon(\omega, q = 0)\}$ [36]. If we want to compare our measurements to any of these techniques then we have to correct our measurements for the contributions with $q \neq 0$. This is equivalent to extracting $\mathrm{Im}\{-1/\epsilon(\omega, q = 0)\}$ from the REELS measurement.

In Ref. [23] Werner et al. tried to deconvolute the $\mathrm{Im}\{-1/\epsilon(\omega, q = 0)\}$ from the measured loss distribution by assuming a free electron like dispersion of the plasmon features and excitation cross sections as given in Eq. (9). As a consequence of the deconvolution the tail at the high-energy loss side of the features decreases and their relative intensity changes (due to different values of θ_e). The results are shown in Fig. 10. Our estimate of $\mathrm{Im}\{-1/\epsilon(\omega, q = 0)\}$ is compared with the optical data given by Palik [24] and the one derived by Daniels [33,37] from transmission electron energy loss.

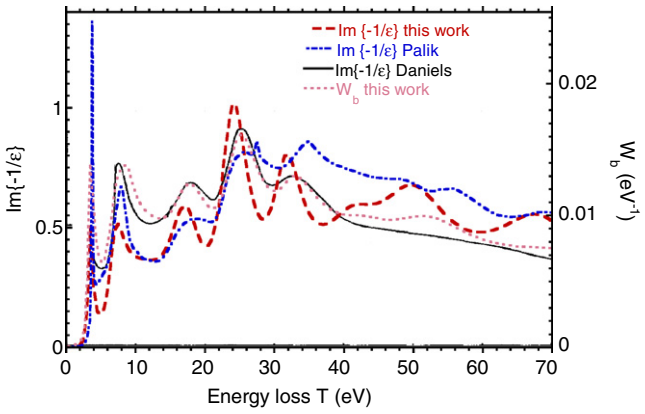

Fig. 10. The loss function $\mathrm{Im}\{-1/\epsilon\}$ (dotted line) obtained in this work, compared $\mathrm{Im}\{-1/\epsilon\}$ derived from optical data (dash-dotted line), as given by Palik [24], and $\mathrm{Im}\{-1/\epsilon\}$ as obtained by Daniels [33] from transmission electron energy loss spectroscopy (black line). Although there are qualitative agreements between the three determinations of $\mathrm{Im}\{-1/\epsilon\}$, quantitatively they are all different. Surprisingly the normalized bulk loss function $W_b(T)$ obtained in this work resembles in shape $\mathrm{Im}\{-1/\epsilon\}$ obtained by Daniels in a transmission electron energy loss experiment very well.

Measurements by Schülter [38] are consistent with Daniels measurements. Qualitatively there are many similarities between the three curves, but quantitatively all three are different. There exist good agreement in shape between our normalized loss function $W_b(T)$ and the transmission EELS determination of $\mathrm{Im}\{-1/\epsilon(\omega, q = 0)\}$ by Daniels. This could be seen as an indication that the transmission EELS measurements are affected by elastic multiple scattering in a similar way as our reflection REELS measurements. Clearly the validity of the procedure used for extracting $\mathrm{Im} - 1/\epsilon(\omega, q = 0)$ from a loss function needs further development and testing.

5. Summary and Conclusion

It is of course impossible to get direct experimental confirmation of the procedure used to extract the volume and surface loss functions (this would make the procedure superfluous), but consistency checks can be done, and comparisons with loss functions obtained with other methods can be made. Here, we summarize the main observations made.

There is fair agreement between the volume and surface loss functions obtained using the two guns. Thus, in spite of the fact that the raw spectra are very different, the obtained surface and bulk loss function obtained for both geometries are fairly consistent. Peak positions are virtually the same, and the intensity reproduces within 10–20%. To what extend the intensity variations are due to shortcomings in the experiment and theory has to be investigated further.

In the high-energy limit the contribution of surface excitations should become vanishing small, and the Tougaard–Chorkendorff procedure should become a valid way to determine the volume loss function. None of the current measurements are close to this limit. However, using the TC procedure for a range of energies we can see that the obtained loss function starts approaching the loss function determined by the procedure described in [21]. The shape of the TC loss function can be described very well using the partial intensity analysis, as given in Eq. (8).

The decomposition procedure suggests that the peak near 3.7 eV is due to both surface and volume excitations. This contrasts to the conclusion reached by Ding et al. that, for the energies they considered (up to 1.5 keV), this feature should be considered as a pure surface excitation [20]. There is quite clear direct experimental evidence that in the present energy range both surface and volume excitations contribute to the 3.7 eV peak:

- The decrease in intensity with increasing energy is slower than what is expected for a pure surface excitation.
- Deposition of Al causes a dramatic reduction of this feature under surface sensitive conditions, but only a marginal decrease in intensity under volume-sensitive conditions, suggesting that in the latter case much of the intensity is due to volume excitations.
- There is a small but clear shift in peak position before and after Al deposition. This shift is in-line with the separation for surface and volume loss features as found experimentally in transmission experiments.

Thus we conclude that the presence of a peak near 3.7 eV in the volume loss function of Fig. 4 is real and not a remnant of the strong surface excitation peak at this energy.

In summary the surface and volume loss functions derived from Ag REELS spectra are consistent with many of the observations made for this well studied system under various conditions both by ourselves and by others. The next important step is the deconvolution of the loss function to extract $\mathrm{Im}\{-1/\epsilon(\omega, q = 0)\}$, and a

Author's personal copy

first attempt was made to do this. Some discrepancies are found between our results of $\mathrm{Im}\{-1/\epsilon(\omega, q = 0)\}$ and those obtained by transmission EELS measurements obtained some time ago at modest energies. It would be helpful if transmission EELS experiments could be done at higher energies (less multiple scattering) and well-defined surface conditions, to provide benchmark results for $\mathrm{Im}\{-1/\epsilon(\omega, q = 0)\}$, that can be used to test the validity of the same quantity extracted from REELS experiments.

References

[1] C.J. Powell, J.B. Swan, Phys. Rev. 118 (1960) 640.
[2] D. Pines, Rev. Mod. Phys. 28 (1956) 184.
[3] R.H. Ritchie, Phys. Rev. 106 (1957) 874.
[4] S. Tougaard, I. Chorkendorff, Phys. Rev. B 35 (1987) 6570.
[5] F. Yubero, S. Tougaard, Surf. Interf. Anal. 19 (1992) 269.
[6] W.S.M. Werner, Phys. Rev. B 71 (2005) 115.
[7] W.S.M. Werner, Surf. Interf. Anal. 37 (2005) 846.
[8] K. Salma, Z. Ding, H. Li, Z. Zhang, Surf. Sci. 600 (2006) 1526.
[9] L. Calliari, M. Dapor, M. Filippi, Surf. Sci. 601 (2007) 2270.
[10] N. Pauly, S. Tougaard, Surf. Sci. 601 (2007) 5611.
[11] F. Yubero, S. Tougaard, Phys. Rev. B 46 (1992) 2486.
[12] C. Denton, J.L. Gervasoni, R.O. Barrachina, N.R. Arista, Phys. Rev. A 57 (1998) 4498.
[13] T.W. Ebbessen, H.J. Lezec, H.F. Ghaemi, T. Thio, P.A. Wolff, Nature 391 (1998) 667.
[14] S.I. Bozhevolnyi, V.S. Volkov, E. Evaux, J.-Y. Laluet, T.W. Ebbesen, Nature 440 (2006) 508.
[15] J. Daniels, Z. Phys. 203 (1967) 235.
[16] E.A. Stern, R.A. Ferrell, Phys. Rev. 120 (1960) 130.
[17] J. Daniels, Z. Phys. 213 (1968) 227.
[18] Y.F. Chen, Surf. Sci. 519 (2002) 115.
[19] W.S.M. Werner, Surf. Sci. 526 (2003) L159.
[20] Z.J. Ding, H.M. Li, Q.R. Pu, Z.M. Zhang, R. Shimizu, Phys. Rev. B 66 (2002) 085411.
[21] W.S.M. Werner, Phys. Rev. B 74 (2006) 075421.
[22] W. Werner, M.R. Went, M. Vos, Surf. Sci. 601 (2007) L109.
[23] W. Werner, M.R. Went, M. Vos, K. Glantschnig, C. Ambrosch-Draxl, Phys. Rev. B 77 (2008) 161404.
[24] E. Palik, Handbook of Optical Constants of Solids, Academic Press, New York, 1985.
[25] M. Vos, G.P. Cornish, E. Weigold, Rev. Sci. Intrum. 71 (2000) 3831.
[26] W.S. Werner, Surf. Sci. 588 (2005) 26.
[27] A. Jablonski, F. Salvat, C.J. Powell, J. Phys. Chem. Ref. Data 33 (2004) 409.
[28] S. Tanuma, C.J. Powell, D.R. Penn, Surf. Interf. Anal. 20 (1993) 77.
[29] W.S.M. Werner, W. Smekal, C. Tomastik, H. Störi, Surf. Sci. 486 (2001) L461.
[30] B. Strawbridge, R.K. Singh, C. Beach, S. Mahajan, N. Newman, J. Vac. Sci. Technol. A 24 (2006) 1776.
[31] C.J. Powell, Phys. Rev. 175 (1968) 972.
[32] R.F. Egerton, Electron Energy-loss Spectroscopy in the Electron Microscope, second ed., Plenum Press, New York, 1996.
[33] J. Daniels, Z. Phys. 227 (1969) 234.
[34] A. vom Felde, J. Sprösser-Prou, J. Fink, Phys. Rev. B 40 (1989) 10181.
[35] A. Otto, E. Petri, Solid State Commun. 20 (1976) 823.
[36] H. Ehrenreich, H.R. Philipp, Phys. Rev. 128 (1962) 1622.
[37] J. Daniels, C. von Festenberg, H. Raether, K. Zeppenfeld, Springer Tracts in Mod. Phys. 54 (1970) 77.
[38] M. Schlüter, Z. Phys. 250 (1972) 87.